American Mineralogist, Volume 95, pages 825–831, 2010

Biodurability of chrysotile and tremolite asbestos in simulated lung and gastric fluids

Christopher Oze* and K'Lynn Solt

Department of Geology, Bryn Mawr College, 101 N. Merion Avenue, Bryn Mawr, Pennsylvania 19010, U.S.A.

Abstract

Chrysotile [$Mg_3Si_2O_5(OH)_4$] and tremolite [$Ca_2Mg_5Si_8O_{22}(OH)_2$] asbestos represent two distinct mineralogical categories of regulated asbestos commonly evaluated in epidemiological, toxicological, and pathological studies. Human respiratory and gastric systems are sites of asbestos deposition where chrysotile and tremolite asbestos are undersaturated with respect to biological fluids and dissolution kinetics control the persistence of these minerals in biological environments. Here we examined the biodurabilities (i.e., the resistance to dissolution) of chrysotile and tremolite asbestos in simulated body fluids as a function of mineral surface area over time. Batch experiments in simulated gastric fluid (SGF; HCl and NaCl solution at pH 1.2) and simulated lung fluid (SLF; modified Gamble's solution at pH 7.4) were performed at 37 °C over 720 h to evaluate the dissolution of chrysotile vs. tremolite asbestos in acidic and near-neutral biological fluids. The rate-limiting step of Si release for both minerals was used to obtain rate constants (k) and reaction orders (n) allowing comparisons of mineral dissolution rates. Both chrysotile and tremolite asbestos are less biodurable in SGF (low pH) compared to SLF (near-neutral pH). Based on equivalent surface area comparisons, the surface chemistry of tremolite is more reactive in lung fluid than chrysotile and vice versa in digestive fluid. However, the relative biodurabilities of these asbestos silicates (from most to least) are tremolite (SLF) > chrysotile (SLF) > tremolite (SGF) > chrysotile (SGF) when accounting for the greater surface area of chrysotile per mass or per fiber compared to tremolite. Overall, this study illustrates the importance of surface area and fiber morphology considerations when evaluating the biodurabilities of asbestiform minerals.

Keywords: Chrysotile, tremolite, serpentine, amphibole, asbestos, dissolution, biodurability

Introduction

Asbestos is a carcinogenic material associated with cancer of the lung (lung cancer and mesothelioma), asbestosis (fibrosis of the lungs), and gastrointestinal cancer (Rom and Palmer 1974; Maresca et al. 1984; Mossman and Churg 1998; Skinner et al. 1988; Holland and Smith 2001; Yano et al. 2001; Roggli et al. 2002; Bernstein et al. 2005, 2006; Pfau et al. 2005; Committee on Asbestos 2006; Plumlee et al. 2006; Gunter et al. 2007; Yarborough 2007). These diseases have been primarily ascribed to the inhalation and ingestion of airborne asbestos particles. Identifying the relationship between asbestos and human toxicity is problematic due to asbestiform minerals having an array of compositions, atomic structural arrangements, and fiber morphologies (i.e., fiber size, length, diameter, and shape) that affect biogeochemical reactions in the body. The multiplicity of potential solution-mineral interactions provides an opportunity to further explore and comparatively evaluate the biodurabilities (i.e., the extent kinetics controls mineral dissolution in body fluids where greater resistance to dissolution makes a material more durable) inherent between two common regulated categories of asbestos: chrysotile (serpentine asbestos; phyllosilicate) and tremolite (amphibole; inosilicate) asbestos. One major factor complicating comparative biodurability evaluations between chrysotile and tremolite asbestos is the greater surface area (per mass or per fiber) of chrysotile compared to tremolite. This surface area discrepancy is a result of chrysotile's "curled sheet" structure compared to tremolite's "needle-like" structure.

The purpose of this study is to develop and compare dissolution rates for chrysotile and tremolite asbestos in biological fluids utilizing mineral surface area considerations that directly reflect bulk mineral-solution interactions governing mineral dissolution. Chrysotile and tremolite asbestos dissolution proceeds via a series of steps involving Si and Mg; however, Si release is the rate-limiting step controlling mineral dissolution rates for both phyllo- and inosilicates (Brantley and Chen 1995; Lasaga 1995; Nagy 1995; Hume and Rimstidt 1992; Jurinski and Rimstidt 2001). In this study, we investigated biodurabilities by monitoring Si release from both chrysotile and tremolite asbestos in simulated body fluids as a function of surface area over time. Batch dissolution experiments were performed at body temperature (37 °C) to examine asbestos biodurabilites in a slightly salty, acidic digestive fluid [simulated gastric fluid (SGF)] juxtaposed to the higher ionic strength, near-neutral pH lung fluid [simulated lung fluid (SLF)]. Although these experiments do not replicate the complexity of the human body and the multitude of processes that may occur, they do provide a benchmark to evaluate the biological breakdown of two mineralogical forms of asbestos at both acidic and near-neutral pHs.

* E-mail: coze@brynmawr.edu

0003-004X/10/0506–825$05.00/DOI: 10.2138/am.2010.3265

Background

The durability of a mineral in any environment, including respiratory and gastric systems, is characterized by its solubility as well as by the rate it will dissolve. Dissolution reactions and equilibrium constants calculated using Geochemist's Workbench (Bethke 1994) for chrysotile [$Mg_3Si_2O_5(OH)_4$] and tremolite [$Ca_2Mg_5Si_8O_{22}(OH)_2$] asbestos at pH values less than 9 and 37 °C are

$$Mg_3Si_2O_5(OH)_4+6H^+ = 3Mg^{2+}+2H_4SiO_4+H_2O \quad K = 10^{30.0} \quad (1)$$

$$Ca_2Mg_5Si_8O_{22}(OH)_2+14H^++8H_2O = 5Mg^{2+}+2Ca^{2+}+8H_4SiO_4 \quad K = 10^{58.6} \quad (2)$$

where the hydrolysis of Mg^{2+} and Ca^{2+} is pH dependent. Both lung and gastric fluids are continually replenished allowing the pHs to be maintained, never exceeding a pH of 8 (Hume and Rimstidt 1992). In human respiratory systems, pH values range from 4 (alveolar macrophage cells), 7 (mesothelial cells), and ~7 (blood plasma), and elemental concentrations for blood plasma and lung tissue are listed in Table 1 (Hume and Rimstidt 1992). Gastric fluid and gastric tissues have pH values ranging from 1.2 (digestive fluid) to 7 (blood plasma), and elemental concentrations for gastric tissue are listed in Table 1 (Iyengar et al. 1978). Note that blood plasma is the most enriched with respect to all the elements of interest (Mg, Ca, and Si as shown in Eq. 1 and Eq. 2). Sodium and Cl are included in Table 1 for ionic strength considerations.

Multiple combinations of fluid-tissue interactions over a range of pHs may occur within the body. To determine whether body fluids and tissues are under- or oversaturated with respect to chrysotile or tremolite asbestos, Visual MINTEQ and its Lindsay thermodynamic database was used to calculate Saturation Index (SI) values (Gustafsson 2006). Negative SI values denote undersaturated fluids/tissues and that mineral dissolution is favorable, whereas positive SI values indicate that fluids are oversaturated and that mineral dissolution will not proceed. All SIs for both chrysotile and tremolite in blood plasma, lung tissue, and stomach tissue using multiple combinations of pH that reflect potential gradients in lung and gastric systems are negative. Thus, both lung and gastrointestinal systems are undersaturated (i.e., mineral dissolution is thermodynamically favorable) with respect to chrysotile and tremolite asbestos, agreeing with other studies (e.g., Hume and Rimstidt 1992; Wood et al. 2006). Ultimately, chrysotile and tremolite asbestos biodurabilities are moderated by their rates of dissolution.

Table 1. Saturation Index (SI) values for chrysotile and tremolite in blood plasma and human lung and stomach tissues over a variety of pH values

Elements	Weighted Mean* (mg/L)	Saturation Index†
Blood Plasma		
		Chrysotile
		pH 1.2: –44.8
Na	3162	pH 4: –27.9
Cl	3610	pH 7:–10.0
Mg	21.2	Tremolite
Si	0.43	pH 1.2: –103.7
Ca	96	pH 4: –64.3
		pH7: –22.3
Lung Tissue		
		Chrysotile
Na	2220×10^{-6}	pH 4: –44.7
Cl	2120×10^{-6}	pH 7: –26.3
Mg	9.84×10^{-3}	Tremolite
Si	57×10^{-6}	pH 4: –116.8
Ca	10.5×10^{-3}	pH 7: –74.7
Gastric-Intestinal Tract Tissue (Stomach)		
		Chrysotile
Na	1000×10^{-6}	pH 1.2: –60.9
Cl	1400×10^{-6}	pH 7: –25.2
Mg	15×10^{-3}	Tremolite
Si	110×10^{-6}	pH 1.2: –154.9
Ca	11×10^{-3}	pH 7: –71.5

* Weighted mean values are from Iyengar et al. (1978).
† Saturation Index (SI) for each mineral was calculated using Visual MINTEQ (Gustafsson 2006) and the Lindsay database.

Materials and methods

Chrysotile (Sample 733; Little Britain Township, Lancaster, Pennsylvania, U.S.A.) and tremolite asbestos (Sample 5034; Harz Mountains, Germany) used in these experiments were obtained from the Bryn Mawr College Rand Mineral Collection (Fig. 1). Mineral identification was accomplished by electron microprobe microanalysis on an automated JEOL 733A electron microprobe (Stanford University's Microanalytical Laboratory) operated at 15 kV accelerating potential and a 15 nA beam current. Calibration was conducted using natural geologic standards. The beam spot was ~1 µm and fiber diameters for both minerals were <10 µm as viewed in backscattered electron images allowing multiple analyses per fiber cross-section. Raw counts were collected over 20 s and were constant with respect to the standards over time indicating that elemental drift was negligible. Detec-

Figure 1. Images of (**a**) chrysotile and (**b**) tremolite asbestos prior to powdering.

tion limits for probe analyses were ~0.02 oxide wt%. The average composition of chrysotile (no. 733) was $Mg_{2.85}Fe_{0.13}Al_{0.02}Si_2O_5(OH)_4$ and the average composition of the tremolite asbestos (no. 5034) was $Ca_{1.97}Mg_{4.69}Fe_{0.28}Mn_{0.02}Al_{0.02}Na_{0.02}Si_8O_{22}(OH)_2$ based on 10 fiber analyses for each sample. Sample mineralogy was confirmed by X-ray diffraction (XRD) using a Rigaku Ultma IV base system with Bragg-Brentano/monochromator capabilities and operating at 40 kV and 40 mA and the JADE software package.

In preparation for the dissolution experiments, chrysotile and tremolite asbestos specimens were ground and powdered in ultrapure water (18.2 MΩ) using an agate mortar and pestle. The ground samples were dried and then rinsed with ultrapure water, rinsed (<30 s) with a 0.01 *N* hydrochloric acid (HCl) solution, and finally rinsed with ultrapure water three more times before drying at room temperature. The acid rinse was performed to minimize high reactivity mineral surface sites created during grinding. Surface area for the prepared chrysotile was 6.14 ± 0.02 m^2/g and for tremolite asbestos, 0.73 ± 0.01 m^2/g as determined using a multipoint N_2 BET isotherm analysis conducted by Micromeritics Analytical Services (MAS).

The simulated lung fluid (SLF) and simulated gastric fluid (SGF) were prepared without enzymes and according to methods used in previous dissolution experiments [(SLF): Moss 1979; Fisher and Briant 1994; Kabe et al. 1996; Heffernan et al. 2001; Jurinski and Rimstidt 2001; LaMont et al. 2001, 2006; (SGF): Polovic et al. 2004; U.S. Department of Health and Human Services 2000; Astwood 2006]. The SLF was composed of 0.101 g/L magnesium chloride ($MgCl_2 \cdot 6H_2O$), 6.019 g/L sodium chloride (NaCl), 0.298 g/L potassium chloride (KCl), 0.268 g/L sodium phosphate ($Na_2HPO_4 \cdot 7H_2O$), 0.071 g/L sodium sulfate (Na_2SO_4), 0.184 g/L calcium choride ($CaCl_2 \cdot 2H_2O$), 0.952 g/L sodium acetate ($NaH_3C_2O_2 \cdot 3H_2O$), 2.604 g/L sodium bicarbonate ($NaHCO_3$), and 0.097 g/L sodium citrate ($Na_3H_5C_6O_7 \cdot 2H_2O$). The SGF was composed of 0.1 *M* hydrochloric acid (HCl) and 2 g/L sodium chloride (NaCl). Silica values were below detection limits (~0.010 mg/kg) in SGF and SLF as determined using inductively coupled plasma optical emission spectrometry (ICP-OES) at Stanford University's Microanalytical Laboratory. Additionally, pHs of the SLF and SGF were ~7.4 and ~1.2, respectively, and did not change throughout the duration of the experiments.

For the batch dissolution experiments, chrysotile and tremolite asbestos were loaded into 50 mL polypropylene sample vials. Each vial contained 0.01, 0.1, or 1.0 g of solid material producing three suspension densities (defined in this study as the surface area per volume of solution, m^2/L; Table 2). A calibrated pipette delivered 20 mL of SGF or SLF into each vial. All variations of suspension density and simulated bodily fluid (SBF) were run in triplicate to obtain the average and standard deviation at one time period. The filled vials were capped and placed in a 37 °C oven to simulate human body temperature. The asbestos-simulated body fluid interactions occurred over four time periods: 24, 120, 360, or 720 h. At the end of each time period the pH of the fluid was analyzed and the fluid was removed using a syringe (terminating the dissolution run/sample) and filtered using a 0.2 µm filter into a clean vial. Samples were acidified using either one drop of concentrated trace metal grade nitric acid (SLF) or concentrated trace metal grade hydrochloric acid (SGF) to suppress surface complexation and precipitation within the fluid. The samples were diluted appropriately and analyzed for Si via ICP-OES at Stanford University's Microanalytical Laboratory.

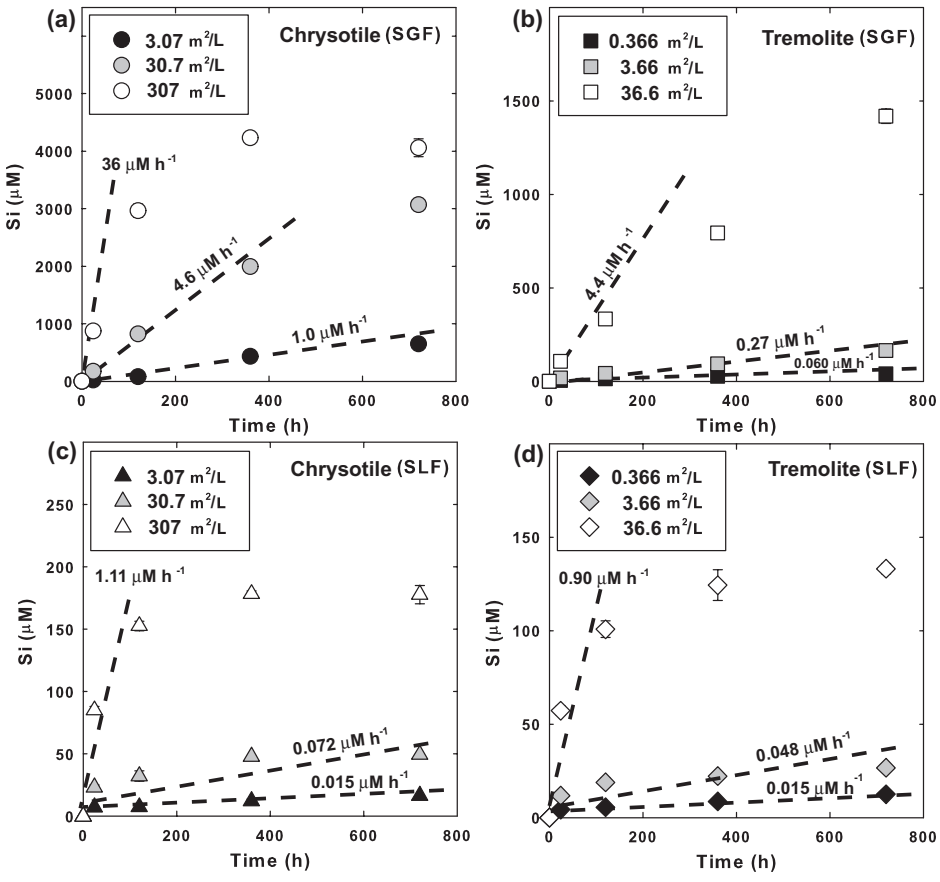

FIGURE 2. Silica release (µM) from chrysotile and tremolite asbestos in simulated gastric fluid (SGF) and in simulated lung fluid (SLF) over time (h) is reported in the following combinations: (**a**) chrysotile-SGF, (**b**) tremolite-SGF, (**c**) chrysotile-SLF, and (**d**) tremolite-SLF. Three suspension densities (m^2/L) for chrysotile (3.07, 30.7, and 307 m^2/L) and tremolite asbestos (0.366, 3.66, and 36.6 m^2/L) were used in both SGF and SLF. Rates of Si release in undersaturated conditions are shown with dashed lines for each suspension density/simulated body fluid run and all R^2 values for linear regressions are >0.9.

TABLE 2. Experimental design for chrysotile and tremolite asbestos batch dissolution experiments

Asbestos	Mass (g)	Surface area (m^2/g)	Total surface area (m^2)	Simulated body fluid (SBF)	Suspension density (m^2/L)	Time periods evaluated (h)
Chrysotile	0.01	6.14	0.0614	20 mL simulated gastric fluid (SGF) per sample	3.07	0, 24, 120, 360, 720
	0.10	6.14	0.614		30.7	0, 24, 120, 360, 720
	1.00	6.14	6.14		307	0, 24, 120, 360, 720
Tremolite	0.01	0.732	0.00732		0.366	0, 24, 120, 360, 720
	0.10	0.732	0.0732		3.66	0, 24, 120, 360, 720
	1.00	0.732	0.732		36.6	0, 24, 120, 360, 720
Chrysotile	0.01	6.14	0.0614	20 mL simulated lung fluid (SLF) per sample	3.07	0, 24, 120, 360, 720
	0.10	6.14	0.614		30.7	0, 24, 120, 360, 720
	1.00	6.14	6.14		307	0, 24, 120, 360, 720
Tremolite	0.01	0.732	0.00732		0.366	0, 24, 120, 360, 720
	0.10	0.732	0.0732		3.66	0, 24, 120, 360, 720
	1.00	0.732	0.732		36.6	0, 24, 120, 360, 720

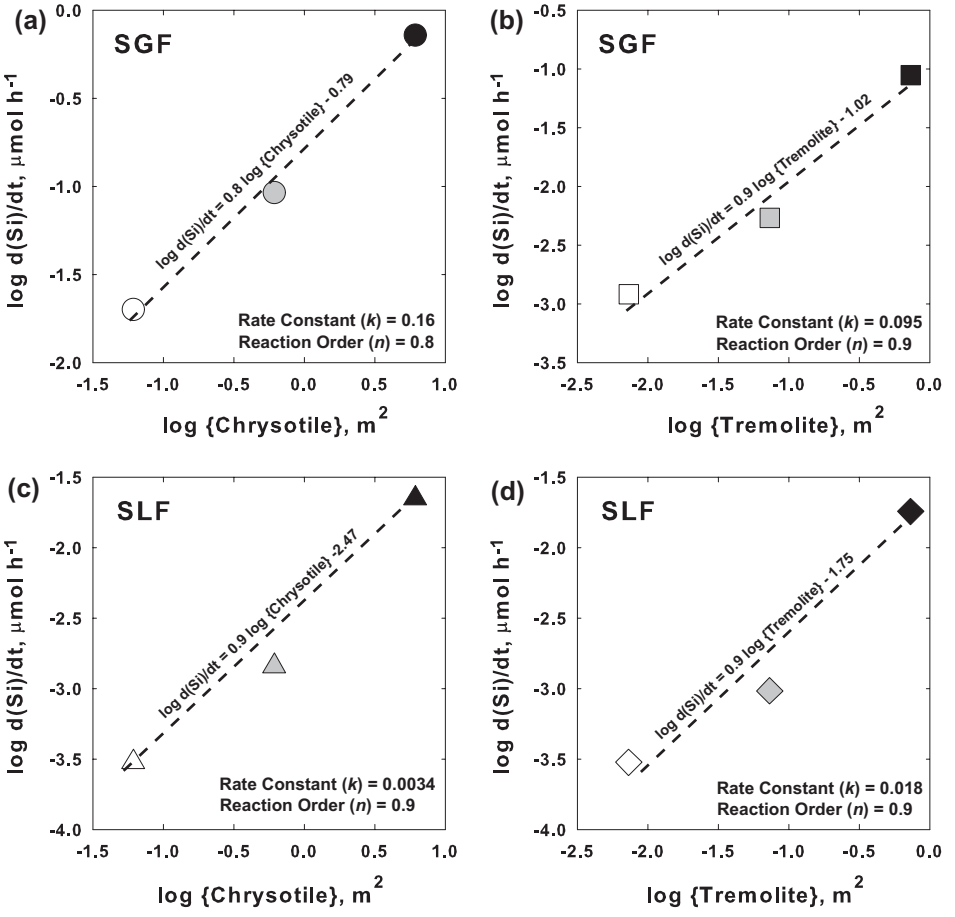

FIGURE 3. Silica release rates (Fig. 1) and surface areas values (Table 1) are incorporated into these logarithmic plots [(**a**) chrysotile-SGF, (**b**) tremolite-SGF, (**c**) chrysotile-SLF, and (**d**) tremolite-SLF] to calculate rate constants (k; µmol $m^{-2\times n}$/h), reaction orders (n), and R^2 values for line fits as shown in Table 4.

RESULTS

Results for Si release from chrysotile and tremolite asbestos in SGF and SLF over time are shown in Figure 2. Generally, as suspension densities (m^2/L) increased, the rate of Si release also increased. Rates of Si release were determined in the undersaturated region (0 to 120 h for the highest suspension densities) of each run to obtain the fastest Si release rate using linear regressions and these rate determinations are shown using dashed lines in Figure 2. Rate values (µM/h) are included in Figure 2. Generally, only the highest suspension densities (chrysotile, 307 m^2/L and tremolite, 36.6 m^2/L) reached saturation (or near-saturation) after 300 h with respect to quartz or amorphous SiO_2 when evaluated using Visual Minteq.

The rate of asbestos dissolution may be assessed using the equation,

$$\frac{d(\mathrm{Si})}{dt} = k_F\{\mathrm{Asbestos}\}^n - k_r\left[\mathrm{Si}\right]^m \quad (3)$$

where $d(\mathrm{Si})/dt$ is the rate (μmol/h) of Si release into solution, k_F is the rate constant (μmol $m^{-2\times n}$/h) of Si release in SGF or SLF, {Asbestos} is the surface area (m^2) for either chrysotile or tremolite asbestos, k_r is the rate constant for a potential back reaction (secondary mineral precipitation, Si adsorption, etc.) involving the concentration of Si, [Si] in solution, and n and m are reaction orders. Figure 1 shows no evidence of Si as a back reactant in the undersaturated region under these experimental conditions; therefore, Equation 3 simplifies to the equation below.

$$\frac{d(\mathrm{Si})}{dt} = k_{\mathrm{SBF}}\{\mathrm{Asbestos}\}^n. \quad (4)$$

To assess rate constants (k) and reaction orders (n) for Si release in relation to surface area, logarithmic rate values of Si release were plotted against their corresponding logarithmic surface areas. Figure 3 uses rates from Figure 2 (converted to units of μmol/h via the 0.020 L solution volume) and surface areas (m^2) from Table 2 to evaluate Si release from both chrysotile and tremolite asbestos in SGF and SLF. Each plot is linearly fit where the slope is equal to the reaction order (n) and the intercept is the log of the rate constant. Rate constants and reaction orders for Si release are reported accordingly in Table 3 with rate constants (k) also being reported in units of mol $m^{(-2\times n)}$/s and reaction orders (n) at ~1. Additionally, line fit values (R^2) for Figure 3 are reported in Table 3 where all R^2 values are greater than 0.93. When accounting for error associated with surface areas and linear regressions, we estimate error for rate constants (k) to be <10%.

DISCUSSION

Using Equation 4 and the rate values reported in Table 3, we are able to compare chrysotile and tremolite asbestos dissolution rates and to evaluate their relative biodurabilities. Overall, Si release rates based on reaction rate constants are ~1 order of magnitude faster in the low pH SGF compared to the near-neutral pH SLF. Based on equivalent surface areas, chrysotile releases Si ~2× faster than tremolite asbestos in SGF; however, tremolite asbestos releases Si ~5× faster than chrysotile in SLF. If comparing Si release rates based on equivalent masses (noting that the surface area per mass of chrysotile is 8.3× larger than that of tremolite; Table 2), chrysotile releases Si faster by a factor of ~1.3 in SLF and by a factor of ~9 in SGF compared to tremolite. These comparisons reflect two different biodurability interpretations where the order and magnitude of chrysotile and tremolite reactivity are dependent on whether equivalent surface areas or masses are considered. If asbestos dissolution is considered at the mesoscopic scale, the most important factor is the difference in morphology between chrysotile and tremolite where the larger surface area per mass of chrysotile dominates the dissolution kinetics. However, dissolution processes at the atomic scale reveal that there is a difference in the reactivity between chrysotile and tremolite surfaces where tremolite is more reactive than chrysotile in SLF and chrysotile is more reactive in SGF. Of more interest, these initial interpretations do not take into account how a fiber may dissolve, which may provide a more robust evaluation of their relative biodurabilities due to including stoichiometric and molar volume considerations.

TABLE 3. Chrysotile and tremolite asbestos dissolution rate constants (k) and reaction orders (n) based on Si release

Asbestos	Simulated bodily fluid	Si rate constant (k) [μmol $m^{(-2\times n)}$/h]	Si rate constant (k) [mol $m^{(-2\times n)}$/s]	Reaction order (n)	R^2 value for line fit
Chrysotile	Gastric	0.16	4.5×10^{-11}	0.8	0.99
	Lung	0.0034	9.3×10^{-13}	0.9	0.98
Tremolite	Gastric	0.095	2.6×10^{-11}	0.9	0.97
	Lung	0.018	4.9×10^{-12}	0.9	0.94

Presently, fiber dissolution models do not realistically account for how a shrinking fiber dissolves with respect to specific crystallographic axes and to preferential dissolution sites capable of modifying fiber morphologies and surface areas. Approximate fiber lifetimes in respiratory and gastric systems can be estimated and compared to distinguish their relative rates of dissolution in respiratory and gastric systems. For assessing fiber dissolution, we use the rate of Si release in relation to number of Si moles present in a 1 μm diameter and 10 μm long fiber. Treating a tremolite fiber as a cylinder will result in a surface area of 33 μm^2 (3.3×10^{-11} m^2). Due to chrysotile typically having a surface area approximately an order of magnitude greater than fibrous tremolite, the chrysotile fiber surface area for this calculation will be 330 μm^2 (3.3×10^{-10} m^2). Additionally, molar volumes and stoichiometries where tremolite is Si-rich (8 Si moles per mole of tremolite) compared to chrysotile (2 Si moles per mole of chrysotile) need to be accounted for to calculate the Si moles in a single fiber. By considering all these factors, fiber lifetimes may be calculated using the equation below:

$$\text{Fiber lifetime} = \begin{bmatrix}\text{Rate of Si release (Eq. 4)}\\ \text{with cylinder surface area}\end{bmatrix}^{-1}\cdot\left(\text{Si μmol in a single fiber}\right) \quad (5)$$

using values shown in Table 4. Using Equation 5 and values in Table 4, a 1 × 10 μm chrysotile fiber will completely dissolve in SLF in ~19 months. A tremolite fiber of equal shape will dissolve in SLF in ~4 years. In SGF, a chrysotile fiber of the same dimensions will dissolve in ~33 h and a tremolite fiber will dissolve in ~9 months. Note, reaction orders (Table 3) used in these calculations have a significant impact on fiber lifetimes where true first-order considerations will alter fiber dissolution rates in Equation 4 and fiber lifetime estimates. Again, these values represent approximate fiber lifetimes and do not account for a shrinking fiber, changes in surface area with respect to time, or for preferential dissolution sites such as crystal defects or edges.

Whether fibers fully dissolve or undergo dissolution for a

TABLE 4. Fiber lifetime estimate of a 1 μm (diameter) × 10 μm (length) cylindrical chrysotile or tremolite fiber (using Eqs. 4 and 5 and Table 3)

Asbestos	Simulated bodily fluid	Surface area (m^2)	Si μmol/h using Equation 4	Cylinder volume (m^3)	Molar volume* (m^3/mol)	Si μmol in a single fiber	Approx. fiber lifetime		
							Hours	Days	Months
Chrysotile	Gastric	3.3×10^{-10}	4.2×10^{-9}	7.9×10^{-18}	1.1×10^{-4}	1.4×10^{-7}	33	1	0
	Lung	3.3×10^{-10}	1.0×10^{-11}	7.9×10^{-18}	1.1×10^{-4}	1.4×10^{-7}	14 000	583	19
Tremolite	Gastric	3.3×10^{-11}	3.5×10^{-11}	7.9×10^{-18}	2.7×10^{-4}	2.3×10^{-7}	6571	274	9
	Lung	3.3×10^{-11}	6.6×10^{-12}	7.9×10^{-18}	2.7×10^{-4}	2.3×10^{-7}	34 848	1452	48

* Robie and Hemingway (1995).

short period of time, the relative dissolution rates will hold true if fiber dissolution is assumed to be simple (i.e., dissolution occurs at the ends or sides of the fiber and the fiber surface area decreases over time). Overall, a chrysotile fiber will dissolve ~200× faster in SLF and ~2.5× faster in SGF compared to tremolite asbestos. Based on our rate constant values and our evaluation of fiber dissolution rates, the relative biodurabilities (resistance to dissolution) of these asbestos silicates (from greatest to least) are tremolite (SLF) > chrysotile (SLF) > tremolite (SGF) > chrysotile (SGF).

Rate constants in Table 3 may also be used to assess particle lifetimes as proposed by Jurinski and Rimstidt (2001) utilizing their spherical shrinking particle model equation

$$t = \frac{d}{2kV_m} \quad (6)$$

where t is time (s), d is the diameter of the spherical particle (m), V_m is the molar volume (m^3/mol), and k is the rate constant (mol m^{-2} s^{-1}). This model overestimates the lifetime of a particle due to the assumption that dissolution occurs evenly over the particle's surface. Using Equation 6 and rate constants (Table 3), a 1 μm spherical particle of chrysotile will have a lifetime of 3.3 years in SGF and 157 years in SLF. A 1 μm spherical particle of tremolite will have a lifetime of 2.3 years in SGF and 12 years in SLF. Using this model, a tremolite sphere will dissolve ~13× faster in SLF and ~1.5× faster in SGF compared to chrysotile. The relative rates at which chrysotile and tremolite dissolve using this model compared to our earlier relative dissolution comparisons are not compatible, especially where tremolite dissolves faster (not slower) in both SLF and SGF. Based on the assumptions and limitations of the shrinking spherical model, this method does not provide an attractive alternative to our earlier fiber dissolution calculations and biodurability comparisons.

These experiments demonstrate that the pH and the solvent chemistry are significant factors affecting the rate of dissolution between chrysotile and tremolite. Our results are in contrast to observations made by Hume and Rimstidt (1992) where chrysotile dissolution rates were independent of pH and solvent chemistry. Additionally, Si release rate constants (k) for chrysotile dissolution are smaller (i.e., slower Si release) for SLF and SGF compared to the average Si release rate constant (5.9×10^{-10} mol m^{-2} s^{-1}) for chrysotile reported by Hume and Rimstidt (1992). The pHs (1.2 and 7.4) and ion-rich solvent (SLF: a modified Gambel's solution) used in our experiments in relation to the more limited pH range (2.06–5.73) of dilute HCl solutions (ionic strengths of 0.12 *m* using NaCl) used by Hume and Rimstidt (1992) possibly account for these discrepancies.

Chrysotile has been noted to be less biodurable than tremolite asbestos in respiratory systems (e.g., Holland and Smith 2001; Fattman et al. 2004; Sporn and Roggli 2004; Plumlee et al. 2006; Wood et al. 2006) and our results agree with these studies when taking into account the greater surface area per mass and per fiber of chrysotile. Data needed to assess the kinetic mechanisms of Si release for chrysotile compared to tremolite, such as analyses from atomic force microscopy (AFM), were not acquired in this study. The overall faster dissolution rates of asbestos in the SGF compared to the SLF may be related to the enhanced effects of H^+ breaking Si-O-Mg connecting O atoms in conjunction with water producing Si-OH and hydrated Mg^{2+} as described by Rosso and Rimstidt (2000). As for ions in solution, the elevated ion concentration in the SLF could potentially minimize the slightly expandable tetrahedral-octahedral (T-O) interlayer spacings (not probable), overwhelm terminal bond sites, or physically affect the "curled" nature of chrysotile, thereby decreasing the reactive surface area and limiting depolymerization reactions. For a concise discussion relevant to evaluating the complexities of magnesium silicate dissolution processes (i.e., the relationship of Mg/Si ratios, mechanisms of dissolution, the effects of mineral structure), please see Jurinski and Rimstidt (2001). Overall, chemical and geometric models do not provide a simple or straightforward way to correlate dissolution rates of magnesium silicates and their respective solutions.

Biological molecules such as proteins not included in these experiments have the potential to modify dissolution reactions for both minerals in lung and digestive fluids potentially shortening fiber lifetimes; however, Jurinski and Rimstidt (2001) determined that organic chelators and proteins did not significantly affect talc dissolution rates. Alternatively, the formation of secondary minerals and chemical adsorption on the fiber's surface will increase the lifetime of a fiber. Ultimately, the duration of fibers to physically remain in the body and react with fluids plays a significant role with regards to how fibers breakdown in the human body and their biodurabilities.

Concluding remarks

The biodurability assessment of chrysotile and tremolite asbestos developed here from surface area reaction kinetics demonstrates the differences inherent between these two forms of asbestos. These experiments reveal that the rates of chrysotile and tremolite dissolution are dependent on pH and solvent chemistry. Both minerals are less biodurable in SGF (low pH) compared to SLF (near-neutral pH). Provided equivalent surface areas, tremolite is less biodurable compared to chrysotile in lung fluid and vice versa in gastric fluid; however, chrysotile is less biodurable in either fluid when taking into account the greater surface area of this mineral or equivalent fiber dimensions. Overall, this study provides supplementary information to aid the future evaluation of naturally occurring asbestos and to provide the relative rates at which they may dissolve in respiratory and gastric systems.

Acknowledgments

This research was funded by the Isabel H. Benham Fund for Faculty Research at Bryn Mawr College. The authors extend their gratitude to Scott Fendorf (Stanford University), Jonas Goldsmith (Bryn Mawr College), Matthew Ginder-Vogel (University of Delaware), Catherine Skinner (Yale University), Mickey Gunter (University of Idaho), Guangchao Li (Stanford University), Josh Landis (Dartmouth College), Ed Ilgren, and an anonymous reviewer for their help, comments, guidance, and expertise.

References cited

Astwood, J.D., Leach, J.N., and Fuchs, R.L. (1996) Stability of food allergens to digestion in vitro. Nature Biotechnology, 14, 1269–1273.

Bernstein, D.M. and Hoskins, J.A. (2006) The health effects of chrysotile: Current perspective based upon recent data. Regulatory Toxicology Pharmacology, 24, 252–264.

Bernstein, D.M., Chevalier, J., and Smith, P. (2005) Comparison of Calidria chrysotile asbestos to pure tremolite: Final results of the inhalation biopersistence and histopathology examination following short-term exposure. Inhalation Toxicology, 17, 427–449.

Bethke, C.M. (1994) The Geochemist's Workbench (Version 2.0): A user's guide to Rxn, Act2, Tact, React, and Gtplot, 213 p. Hydrogeology Program, University of Illinois.

Brantley, S.L. and Chen, Y. (1995) Chemical weathering rates of pyroxenes and amphiboles. In A.F. White and S.L. Brantley, Eds., Chemical Weathering Rates of Silicate Minerals, 31, p. 118–172. Reviews in Mineralogy, Mineralogical Society of American, Chantilly, Virginia.

Committee on Asbestos: Selected Health Effects (2006) Asbestos: Selected cancers, 340 p. National Academies Press, Washington, D.C.

Fattman, C.L., Chu, C.T., and Oury, T.D. (2004) Experimental models of asbestos-related diseases. In V.L. Roggli, T.D. Oury, and T.A. Sporn, Eds., Pathology of Asbestos-Associated Diseases, 2nd edition, p. 256–308. Springer, Berlin.

Fisher, D.R. and Briant, J.K. (1994) Assessment of accidental intakes of uranyl acetylacetonate (UAA). Radiation Protection Dosimetry, 53, 263–267.

Gunter, M.E., Belluso, E., and Mottana, A. (2007) Classification of the amphiboles. In F.C. Hawthorne, R. Oberti, G.D. Ventura, and A. Mottana, Eds., Amphiboles: Crystal Chemistry, Occurrence, and Health Issues, 67, p. 453–516. Reviews in Mineralogy and Geochemistry, Mineralogical Society of America, Chantilly, Virginia.

Gustafsson, J.P. (2006) Visual MINTEQ 2.51. Department of Land and Water Resources Engineering, KTH, Stockholm, Sweden.

Heffernan, T.E., Lodwick, J.C., Spitz, H., Neton, J., and Soldano, M. (2001) Solubility of airborne uranium compounds at the Fernald environmental management project. Health Physics, 80, 255–262.

Holland, J.P. and Smith, D.D. (2001) Asbestos. In J.B. Sullivan Jr. and G. Kreiger, Eds., Clinical Environmental Health and Exposures, 2nd edition, p. 1214–1227. Lippincott Williams and Wilkins, Philadelphia.

Hume, L.A. and Rimstidt, J.D. (1992) The biodurability of chrysotile asbestos. American Mineralogist, 77, 1125–1128.

Iyengar, G.V., Kollmer, W.E., and Bowen, H.J.M. (1978) The Elemental Composition of Human Tissues and Body Fluids, 363 p. Verlag Chemie, New York.

Jurinski, J.B. and Rimstidt, J.D. (2001) Biodurability of talc. American Mineralogist, 86, 392–399.

Kabe, I., Omae, K., Nakashima, H., Nomiyama, T., Uemura, T., Hosoda, K., Ishizuka, C., Yamazaki, K., and Sakurai, H. (1996) In vitro solubility and in vivo toxicity of indium phosphide. Journal of Occupational Health, 38, 6–12.

LaMont, S.P., Maddison, A.P., Filby, R.H., and Glover, S.E. (2001) Determination of the in vitro dissolution rates of ^{238}U, ^{230}Th, and ^{231}Pa in contaminated soils from the St. Louis FUSRAP sites. Journal of Radioanalytical and Nuclear Chemistry, 248, 509–515.

LaMont, S.P., Labone, T.R., Cadieux, J.R., Findley, W.M., Hall, G., Shick, C.R., Efurd, D.W., and Steiner, R.E. (2006) In vitro lung dissolution rates for PuO_2. Journal of Radioanalytical and Nuclear Chemistry, 269, 271–277.

Lasaga, A.C. (1995) Fundamental approaches in describing mineral dissolution and precipitation rates. In A.F. White and S.L. Brantley, Eds., Chemical Weathering Rates of Silicate Minerals, 31, p. 23–86. Reviews in Mineralogy, Mineralogical Society of America, Chantilly, Virginia.

Maresca, G.P., Puffer, J.H., and Germain, M. (1984) Asbestos in lake and reservoir waters of Staten Island, New York: Source, concentration, mineralogy, and size distribution. Environmental Geology Water Science, 6, 201–210.

Moss, O.R. (1979) Simulants of lung interstitial fluid. Health Physics, 36, 447–448.

Mossman, B.T. and Churg, A. (1998) Mechanisms in the pathogenesis of asbestosis and silicosis. American Journal of Respiratory and Critical Care Medicine, 157, 1666–1680.

Nagy, K.L. (1995) Dissolution and precipitation kinetics of sheet silicates. In A.F. White and S.L. Brantley, Eds., Chemical Weathering Rates of Silicate Minerals, 31, p. 173–233. Reviews in Mineralogy, Mineralogical Society of America, Chantilly, Virginia.

Pfau, J.C., Sentissi, J.J., Weller, G., and Putnam, E.A. (2005) Assessment of autoimmune responses associated with asbestos exposure in Libby, Montana, U.S.A. Environmental Health Perspectives, 113, 25–30.

Plumlee, G.S., Morman, S.A., and Ziegler, T.L. (2006) The toxicological geochemistry of earth minerals: An overview of processes and the interdisciplinary methods used to understand them. In N. Sahai and M.A.A. Schoonen, Eds., Medical Mineralogy and Geochemistry, 64, p. 5–57. Reviews in Mineralogy and Geochemistry, Mineralogical Society of America, Chantilly, Virginia.

Polovic, N.D., Cirkovic-Velickovic, T.D., Gavroic-Jankulovic, M.D., Burazer, L., Dergovic-Petrovic, D., Vuckovic, O., and Jankov, R.M. (2004) IgG binding of mugwort pollen allergens and allergoids exposed to simulated gastrointestinal conditions measured by a self-developed ELISA Test. Journal of the Serbian Chemical Society, 69, 533–540.

Robie, R.A. and Hemingway, B.S. (1995) Thermodynamic properties of minerals and related substances at 298.15 K and 1 bar (105 Pascals) pressure and at higher temperatures. U.S. Geological Survey Bulletin 2131, 461 p.

Roggli, V.L., Vollmer, R.T., Butnor, K.J., and Sporn, T.A. (2002) Tremolite and mesothelioma. Annals of Occupational Hygiene, 46, 447–453.

Rom, W.M. and Palmer, P.E.S. (1974) The spectrum of asbestos related diseases. Western Journal of Medicine, 121, 10–21.

Rosso, J.J. and Rimstidt, J.D. (2000) A high resolution study of forsterite dissolution rates. Geochimica et Cosmochimica Acta, 64, 797–811.

Skinner, C.H., Ross, M., and Frondel, C. (1988) Asbestos and other fibrous materials: Mineralogy, crystal chemistry, and health effects, 222 p. Oxford University Press, New York.

Sporn, T.A. and Roggli, V.L. (2004) Mesothelioma. In V.L. Roggli, T.D. Oury, and T.A. Sporn, Eds., Pathology of Asbestos-Associated Diseases, 2nd edition, p. 104–168. Springer, Berlin.

U.S. Department of Health and Human Services (2000) Waiver of in vivo bioavailability and bioequivalence studies for immediate-release solid oral dosage forms based on a biopharmaceutics classification system. Food and Drug Administration, Center for Drug Evaluation Research, http://www.fda.gov/downloads/Drugs/GuidanceComplianceRegulatoryInformation/Guidances/ucm070246.pdf.

Wood, S.A., Taunton, A.E., Normand, C., and Gunter, M.E. (2006) Mineral-fluid interaction in the lungs: Insights from reaction-path modeling. Inhalation Toxicology, 18, 975–984.

Yano, E., Wang, Z.M., Wang, X.R., Wang, M.Z., and Lan, Y.J. (2001) Cancer mortality among workers exposed to amphibole-free chrysotile asbestos. American Journal of Epidemiology, 154, 538–43.

Yarborough, C.M. (2007) The risk of mesothelioma from exposure to chrysotile asbestos. Current Opinion in Pulmonary Medicine, 13, 334–338.

Manuscript received April 2, 2009
Manuscript accepted January 19, 2010
Manuscript handled by Pupa Gilbert